[CANCER RESEARCH 64, 4171–4179, June 15, 2004]

αCP-4, Encoded by a Putative Tumor Suppressor Gene at 3p21, But Not Its Alternative Splice Variant αCP-4a, Is Underexpressed in Lung Cancer

Ruben Pio,[1,2] Isabel Zudaire,[1,3] Irene Pino,[1,4] Zafira Castaño,[1] Natalia Zabalegui,[5] Silvestre Vicent,[1,4] Fermin Garcia-Amigot,[5] Maria D. Odero,[1,3] Maria D. Lozano,[4] Jesus Garcia-Foncillas,[5] Maria J. Calasanz,[3] and Luis M. Montuenga[1,4]

[1]Division of Oncology and Departments of [2]Biochemistry, [3]Genetics, [4]Histology and Pathology, and [5]Biotechnology, Clinica Universitaria and School of Medicine, Center for Applied Medical Research. University of Navarra. Pamplona, Spain

ABSTRACT

αCP-4 is an RNA-binding protein coded by *PCBP4*, a gene mapped to 3p21, a common deleted region in lung cancer. In this study we characterized the expression of αCP-4 and αCP-4a, an alternatively spliced variant of αCP-4, in lung cancer cell lines and non-small cell lung cancer (NSCLC) samples from early stage lung cancer patients. In NSCLC biopsies, an immunocytochemical analysis showed cytoplasmic expression of αCP-4 and αCP-4a in normal lung bronchiolar epithelium. In contrast, αCP-4 immunoreactivity was not found in 47% adenocarcinomas and 83% squamous cell carcinomas, whereas all of the tumors expressed αCP-4a. Besides, lack of αCP-4 expression was associated with high proliferation of the tumor (determined by Ki67 expression). By fluorescence *in situ* hybridization, >30% of NSCLC cell lines and tumors showed allelic losses at *PCBP4*, correlating with the absence of the protein. On the other hand, no mutations in the coding region of the gene were found in any of the 24 cell lines analyzed. By Northern blotting and real-time reverse transcription-PCR, we detected the expression of αCP-4 and αCP-4a messages in NSCLC and small cell lung cancer cell lines. Our data demonstrate an abnormal expression of αCP-4 in lung cancer, possibly associated with an altered processing of the αCP-4 mRNA leading to a predominant expression of αCP-4a. This may be considered as an example of alternative splicing involved in tumor suppressor gene inactivation. Finally, induction of αCP-4 expression reduced cell growth, in agreement with its proposed role as a tumor suppressor, and suggesting an association of this RNA-binding protein with lung carcinogenesis.

INTRODUCTION

Cytogenetic analyses have established that genetic alterations on the short arm of chromosome 3 are among the most common abnormalities found in lung cancer. Loss of heterozygosity (LOH) at 3p, frequently at 3p21, occurs at the very earliest preneoplastic stages and has been also shown in histologically normal bronchial epithelium from patients with lung cancer and smokers without cancer (1–3). It has been repeatedly hypothesized that persistent 3p21 LOH in lung cancer may indicate that this area harbors one or more tumor suppressor genes of which the inactivation is required for malignant transformation. This region has been extensively examined to characterize these tumor suppressor genes (4, 5). Although some candidates have been suggested (6–8), the identification of tumor suppressor genes has proven elusive, and intense research efforts are currently devoted to this task. As part of this effort, in a detailed allelotyping analysis in tumors and tumor cell lines, multiple areas of discontinuous LOH throughout the 3p21 region were identified (4).

PCBP4 is located at 3p21 and codes for αCP-4, a member of the polycytidylic acid binding protein (PCBP) family. PCBPs are RNA-binding proteins characterized by a high polycytidylic acid affinity. These are composed of two subsets in mammalian cells, hnRNPs K/J and αCP proteins (9). The best-characterized αCP members are αCP-1 and αCP-2. These proteins are involved in several aspects of post-transcriptional gene regulation (9). On the basis of sequence similarity, two novel αCP proteins, denoted as αCP-3 and αCP-4, have been characterized (10). Almost simultaneously to the report identifying the new members of the αCP family, a novel cellular p53 target named MCG10 was found (11). When MCG10 expression was induced in lung cancer cells they underwent apoptosis and cell cycle arrest in G_2-M (11). Because MCG10 mapped to 3p21, the authors suggested its potential role as a new tumor suppressor gene (11). Sequence identity demonstrates that both αCP-4 and MCG10 are the same protein, although with some discrepancies at the NH_2 terminus sequence (9). One alternatively spliced form of αCP-4 has been described. This alternative form, termed αCP-4a, differs from αCP-4 in length and primary sequence at the COOH terminus (10). Whereas no data on the intracellular localization of αCP-4 exist, immunofluorescence studies have revealed that αCP-4a expression is restricted to the cytoplasm in transfected HeLa cells (12).

In view of all of these data, we aimed to characterize the expression of αCP-4 and its alternatively spliced form αCP-4a in normal lung and lung cancer to better evaluate its implication in lung carcinogenesis. We studied the expression of αCP-4 and αCP-4a mRNA and protein in lung cancer cell lines and NSCLC biopsies, respectively. This expression was compared with that in normal lung tissue and abnormal histological lesions such as epithelial hyperplasias. Because allelic losses are accepted as a preliminary indication of tumor suppressor gene inactivation, we determined the frequency of losses at *PCBP4* locus in cancer cell lines [both small cell lung cancer (SCLC) and non-small cell lung cancer (NSCLC)] and NSCLC biopsies. We also searched for mutations on the coding domain sequence of the gene. Our results showed frequent lack of αCP-4 protein expression (predominantly in squamous cell carcinomas) associated with *PCBP4* allele loss. Subsequently, the lack of αCP-4 was associated with poorly differentiated and highly proliferative tumors. No mutations were found in any of the lung cancer cell lines analyzed. Surprisingly, the expression of αCP-4a, the other protein derived from *PCBP4* by alternative splicing, was apparently normal in lung tumors. We also confirmed the decrease in growth rate induced by αCP-4 expression. Taken together, our results indicate a possible role of αCP-4 in lung carcinogenesis and suggest the involvement of an RNA metabolism-related mechanism for inhibiting the expression of this protein.

MATERIALS AND METHODS

Cell Lines. A range of lung cancer cell lines from the American Type Culture Collection (Manassas, VA) were used. Cells were grown in RPMI 1640 supplemented with 10% fetal bovine serum and penicillin-streptomycin (Invitrogen, Carlsbad, CA). Cell lines included in the study were as follows: SCLC (H69, H82, H187, H345, H446, H510, N417, H209, and H774), adenocarcinoma (H23, H676, Calu-3, H1264, H441, and H2087), bronchi-

Received 9/22/03; revised 2/26/04; accepted 3/24/04.

Grant support: "UTE project CIMA," and Fondo de Investigaciones Sanitarias (# 00/0835 and PI021116), Red Temática de Investigación Cooperativa de Centros de Cáncer del Ministerio de Sanidad y Consumo (# C03/10), and Departamento de Salud del Gobierno de Navarra (# 38/2003).

The costs of publication of this article were defrayed in part by the payment of page charges. This article must therefore be hereby marked *advertisement* in accordance with 18 U.S.C. Section 1734 solely to indicate this fact.

Requests for reprints: Ruben Pio, Department of Biochemistry, School of Medicine, University of Navarra, Irunlarrea 1, Pamplona 31080, Spain. Phone: 34-948-425600. Fax: 34-948-425649. E-mail: rpio@unav.es.

oloalveolar carcinoma (A549), squamous cell carcinoma (HTB-58, H157, and H226), large cell carcinoma (H661, H1385, and H1299), and carcinoid (H720 and H727). Primary cultures of normal human bronchial epithelial cells (Clonetics, San Diego, CA) grown in supplemented epithelial cell growth media (BGEM; Clonetics) were also used.

Lung Cancer Biopsies. Lung carcinoma samples were obtained under an institution-approved human tissue procurement protocol. The patients consisted of 5 females and 28 males ranging in age from 45 to 87 years (mean age, 62 years). All of them were current or former smokers except for 1. Most of them were patients at early stages in the moment of diagnosis (22 stage I, 7 stage II, 3 stage III, and 1 stage IV). The tumors consisted of 18 squamous cell carcinomas and 15 adenocarcinomas (including 4 bronchioloalveolar carcinomas). Tumors, adjacent areas to the tumor, and distant (usually >5 cm) normal uninvolved tissue were obtained. Samples were immersed in buffered formalin within 20 min from surgical resection. All of the samples were removed from the fixative solution after 24 h fixation. Tissues were paraffin embedded and sectioned (3 μm).

Antibody Production and Characterization. Rabbit polyclonal antibodies against αCP-4 and αCP-4a were generated by Zymed Laboratories (San Francisco, CA). Specific COOH-terminal sequences of αCP-4 [peptide sequence (C)NGSKKAERQKFSPY] and αCP4a [peptide sequence (K)GLGGLHCQDGSS] were used for immunization. Antibodies were purified from sera by affinity chromatography after coupling of the peptides to the column gel (Sulfo Link Coupling Gel; Pierce, Rockford, IL). Pure antibodies were stored in phosphate buffer saline at 1 mg/ml. The characterization of the immunoreactivity was carried out by ELISA using the immobilized peptides. Western blotting with protein extracts from a cell line transfected with αCP4 or αCP4a cDNA showed the specificity of each antibody in the recognition of each variant.

Immunocytochemistry. Biopsy sections (3 μm) from all of the patients were deparaffinized and incubated overnight at 4°C with a 1:1000 dilution of the rabbit polyclonal antibodies against αCP-4 or αCP-4a. After applying the ENVISION system (DAKO, Carpinteria, CA) for 30 min, the immunostaining was developed with diaminobenzidine and counterstained with Harris hematoxylin. Ki67 and p53 immunostaining were carried out using the monoclonal antibodies MM1 and DO-7, respectively (Novocastra Laboratories, Newcastle, United Kingdom). Tissue sections were microwaved at pH 6 for 15 min at highest power (1150 W) and 15 min at lowest power (700 W) to unmask the antigen. Sections were incubated overnight at 4°C with the primary antibody (MM1 diluted 1:100 or DO-7 diluted 1:80). For p53 immunostaining, the ENVISION system (DAKO) and the diaminobenzidine detection solution were applied. In the case of Ki67 immunostaining, we used a secondary antibody (1:200) containing rabbit antimouse IgG (DAKO) for 30 min, followed by an incubation with avidin-biotin complexes (DAKO). Adsorption of αCP-4 or αCP-4a antibodies in the presence of the synthetic peptides (10 μM) was used to confirm the specificity of the immunostaining.

Fluorescence *in Situ* Hybridization (FISH). FISH analysis was performed in 21 primary tumors and the following lung cancer cell lines: H69, H82, H187, H345, H446, N417, H23, Calu-3, H1264, H441, A549, HTB-58, H157, H720, and H727. Tissue sections were obtained as indicated previously. Cultured cell lines were treated for 4 h with 0.01 g/ml Colcemid (Life Technologies, Inc., Gaithersburg, MD), treated with a hypotonic solution of 75 mM KCl, and fixed in 3:1 methanol:acetic acid. Two-color FISH analysis was performed with bacterial artificial chromosome RP11–314A5, which includes *PCBP4*, and with a fluorescein direct-labeled chromosome 3 centromeric probe (Qbiogene, GmbH, Heidelberg, Germany) used as control. Bacterial artificial chromosome DNA was labeled with SpectrumOrange fluorochrome (Vysis, Downers Grove, IL) by nick-translation. The localization of the bacterial artificial chromosome probe was verified by FISH on normal lymphocyte metaphases. FISH analysis was carried out as follows. Deparaffined tissue sections were pretreated with 30% sodium bisulfite (20 min at 45°C) and digested with 0.25 mg/ml proteinase K (10 min at 45°C) followed by ethanol dehydration. In the cell lines, slides were incubated in 2× SSC at 37°C for 15 min before ethanol dehydration. Samples and probes were denatured at 75°C (5 min and 12 min, respectively), and hybridization was performed at 37°C for 2 days. Posthybridization washes were performed at 73°C for 2 min in 2× SSC/0.3% NP40 and then samples were counterstained with DAPI II (Vysis). Slides were evaluated using a Zeiss Axioplan2 fluorescence microscope. To analyze tumor sections, the areas of neoplastic cells were determined by evaluating the adjacent sections with H&E staining. FISH signals were counted from 200 nuclei of the tumor regions, and the average ratio between the number of signals for the gene probe and the number of signals for the centromeric probe was calculated. Cut-offs were calculated as the mean percentage of false deletions/gains in normal cells plus three times the SD.

Mutation Analysis. Exons 2–13 of *PCBP4*, the αCP-4 gene (accession no. 29793768), were sequenced using the Big Dye Terminator V1.1 Cycle Sequencing kit (Applied Biosystems, Foster City, CA). Genomic DNA from 24 lung cancer cell lines (15 NSCLC and 9 SCLC) was subjected to PCR amplification with a set of intronic primers flanking each exon. The PCR products were sequenced according to the protocol supplied by the manufacturer using an internal primer. The sequencing reactions were carried out in a Gene Amp PCR System 2400, and final products were processed with the ABI Prism377 DNA sequencer. Software used to analyze the results was ABI Prism377XL Collection, Sequence Navigator 1.0.1 and Sequencing Analysis 3.4.1.

Northern Blotting. Total RNA was isolated from the cell lines using the guanidine isothiocyanate and cesium chloride method (13). Fifteen μg of RNA were loaded per lane, run in 1% agarose gels containing 2.2 M formaldehyde, blotted onto nitrocellulose membranes, and baked for 2 h at 80°C. Equal loading and integrity of RNA were monitored by ethidium bromide staining of the 28 S subunit of rRNA. The human αCP4 cDNA probe (883 pb) used in this study was generated from a reverse transcription-PCR (RT-PCR) product cloned into the pDONR-201 vector (Invitrogen) and digested using *Sac*I and *Xba*I. The oligonucleotide primers used for the amplification were αS-1 and αAS-1. All of the sequences of these and other primers used throughout the study are shown in Table 1. The location of the primers and probes are shown in Fig. 1. The RT-PCR product was sequenced to validate the integrity of the probe. Probe was labeled with [α-^{32}P]dCTP (3000 Ci/mmol; NEN Life Science Products, Boston, MA) using the Prime-it RmT Random Primer Labeling kit (Stratagene, La Jolla, CA). Unincorporated nucleotides were removed by MicroSpin G-50 Columns (Amersham Pharmacia Biotech, Piscataway, NJ). Hybridization was carried out overnight at 42°C in a hybridization buffer containing 40% formamide (13). After stringency washes, blots were exposed to X-ray films for various times.

Table 1 *Primers and probes*

Name	Sequence (5′→3′)	Position[a]
αS-1	ACAGAATGAGCGGCTCGGACGGGGGA	143–168 (sense)
αAS-1	CTCAGTAGGGGGAGAATTTCTGCCG	1336–1360 (antisense)
αS-2	AGCTCTCAAGCCATGCGGTC	800–819 (sense)
αAS-2	TTTCTGCCGCTCAGCCTTCTT	1324–1344 (antisense)
αS-3	TGCCCTTCTTGGCTTTACCA	1235–1254 (sense)
αAS-3	CCATTAGCTGCTGCCATCTTG	1299–1319 (antisense)
αS-4	ATCGCCCTGGCCCAGTAC	1039–1056 (sense)
αAS-4	CCATTAGCTGCTGCCATCTTG	1299–1319 (antisense)
GAPDH-S[b]	GAAGGTGAAGGTCGGAGTC	66–84 (sense)
GAPDH-AS	GAAGATGGTGATGGGATTTC	272–291 (antisense)
αP-3	(Fam)-CTGCTTCCCCAGGGCCGCC-(Tamra) (phosphate)	1256–1274 (sense)
αP-4	(Fam)-CCGGGCTTGGCGGCCTACA-(Tamra) (phosphate)	1276–1294 (sense)
GAPDH-P	(Joe)-CAAGCTTCCCGTTCTCAGCC-(Tamra) (phosphate)	243–261 (sense)

[a] Numbering of the nucleotide base positioning was taken from the GenBank profile accession numbers NM_033010 (human αCP-4 mRNA) and M33197 (human GAPDH mRNA).
[b] GAPDH, glyceraldehyde-3-phosphate dehydrogenase; Fam, carboxyfluorescein; Tamra; 6-carboxytetramethylrhodamine.

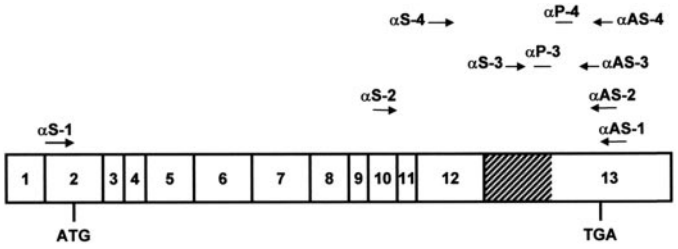

Fig. 1. Scheme representing the αCP-4 cDNA structure (10) and the location of the primers and probes used in the study. The shadowed area represents the alternatively spliced sequence that originates αCP-4a.

Real-Time Semiquantitative RT-PCR. Semiquantitative analysis of the αCP-4 mRNA expression was carried out by real-time RT-PCR with the ABI PRISM 7700 Sequence Detector and the software Sequence Detector version 1.6.3. (Perkin-Elmer/Applied Biosystems, Foster City, CA). RNA was isolated from all of the cell lines using the guanidine isothiocyanate and cesium chloride method. The reactions were performed with 2 μg of total RNA with minor differences from ABI 7700 manufacturer's instructions. Relative levels of expression were determined by the Ct method. Every assay was performed in triplicate. For a separated quantification of αCP4 and αCP4a we designed specific primers for each variant (Table 1; Fig. 1). Primers for αCP-4 mRNA amplification were αS-3 and αAS-3 with the internal TaqMan probe for the amplified sequence denoted as αP-3. The primers and probe specific for αCP4a variant were αS-4, αAS-4, and αP-4. All of the experiments included a glyceraldehyde-3-phosphate dehydrogenase internal standard. The sequences of the primers and probe used for glyceraldehyde-3-phosphate dehydrogenase amplification are shown in Table 1. Semiquantitative mRNA levels were expressed as a percentage relative to the glyceraldehyde-3-phosphate dehydrogenase mRNA.

Cell Growth Assay. H1299 cells that inducibly express αCP-4 or αCP4a were generated as follows. Full-length αCP-4 or αCP-4a cDNA was cloned into a retroviral vector (pLTR) containing the two components of the reverse tetracycline-regulated system (14). H1299 cells were infected with the retrovirus as described (14). The effect of αCP-4 or αCP-4a overexpression on cell growth was studied using the 3-(4,5-dimethylthiazol-2-yl)-2,5-diphenyltetrazolium bromide-based colorimetric assay cell growth proliferation kit (Roche, Mannheim, Germany). Briefly, cells were seeded at a density of 1×10^3 cells/well in 100 μl of culture medium into 96-well plates and allowed to adhere. The next day, expression of the protein was induced with doxycycline (1 mg/ml). Growth was measured daily up to 6 days, replacing the medium after 3 days of incubation. At each day, 10 ml of the 3-(4,5-dimethylthiazol-2-yl)-2,5-diphenyltetrazolium bromide-labeling reagent were added per well. After incubation for 4 h, the solubilization solution (100 μl) was added to each well, and the plate was additionally incubated overnight. Absorbance was measured using a microtiter plate reader.

Statistical Analysis. Qualitative data obtained from the biopsies were analyze by Kendall's correlation test. Data obtained from the 3-(4,5-dimethylthiazol-2-yl)-2,5-diphenyltetrazolium bromide growth assay were analyzed by Student's *t* test. A $P < 0.05$ was considered to be significant.

RESULTS

***α*CP-4 Expression in Lung Cancer Biopsies.** To characterize the αCP-4 expression in biopsies we developed a polyclonal antibody specific for the COOH-terminal sequence of the protein. By immunocytochemistry, we analyzed biopsies from 33 NSCLCs, 15 adenocarcinomas, and 18 squamous cell carcinomas. We determined the presence of αCP-4 in both cancer cells and uninvolved lung tissue (Fig. 2, *A–F*). In normal lung bronchial epithelium a noticeable granular cytoplasmic expression, mostly in the apical region, was observed (Fig. 2, *A* and *B*). In contrast, normal alveoli showed no immunoreactivity. In the case of malignant tissue, 67% of cases lacked αCP-4 expression (47% adenocarcinomas and 83% squamous cell carcinomas). As observed in normal bronchioli, the location of the protein was cytoplasmic in the positive tumors (Fig. 2*F*), except for 1 adenocarcinoma in which a moderate nuclear staining was also detected. Interestingly, in hyperplastic bronchiolar epithelial tissue the protein was absent (Fig. 2*C*), except for 1 case in which we found a positive hyperplastic bronchiole next to an adenocarcinoma also expressing the protein. In areas of dysplasia found in our series, expression of αCP-4 was not found. On the other hand, there was an inverse correlation (Kendall's τ-b coefficient = 0.507; $P = 0.001$) between the presence of αCP-4 in the tumors and their proliferative status determined by Ki67 expression (Fig. 3). A highly significant correlation (Kendall's τ-b coefficient = 0.509; $P < 0.001$) was also found between the expression of αCP-4 and the histological grade of the tumor, where poorly differentiated tumors were associated to loss of αCP-4. Although αCP-4 has been identified as a p53 target gene, no correlation was found between αCP-4 expression and abnormal nuclear accumulation of p53, assessed by immunocytochemistry techniques (Kendall's τ-b coefficient = 0.069; $P = 0.720$).

Status of PCBP4. Deletion at *PCBP4* was determined by FISH using bacterial artificial chromosome RP11314-A5 labeled with SpectrumOrange. A fluorescein-labeled chromosome 3 centromeric probe was used as control. To established the cutoff of false deletion/gain results in the biopsies we carried out FISH analysis of 5 normal-appearing bronchiolar epithelial areas coming from the histologically normal regions of the samples from which tumors were obtained. For cell lines, blood samples from 5 healthy donors were also used as controls. Cutoff was calculated as mean percentage of false deletions/gains in controls plus three times the SD. In tissue sections, the percentage of false deletions (percentage of normal nuclei with a ratio below 1) was 12.4 ± 6.4 (mean ± SD), and thus a cutoff of 31.6% was used. This implies that tumors showing <31.6% of nuclei with a ratio below 1 were considered normal, whereas tumors with >31.6% of their nuclei with a ratio below 1 were considered to have *PCBP4* deletion. On the other hand, percentage of normal nuclei with a ratio >1 (false gain) was 11.1 ± 5.1 (cutoff for gains 26.4%). In cell lines, the cutoff level for deletion was 4.1 (1.7 ± 0.8) and for gain was 5.4% (2.6 ± 0.95). Fifteen cell lines (both SCLC and NSCLC cell lines) were analyzed. The G banding analysis revealed complex karyotypes with structural rearrangements and frequent polyploidy. FISH analysis in SCLC cell lines showed *PCBP4* allele deletion in H446, whereas H69, H82, H187, N417, and H345 were normal. In NSCLC cell lines, 4 of them showed deletion at *PCBP4* (H23, A549, H720, and H441), 4 were normal (H1264, H727, HTB-58, and Calu-3), and in 1 case (H157) a gain of the gene was detected. In the NSCLC biopsies, 21 cases could be analyzed. One of 10 adenocarcinomas and 6 of 11 squamous cell carcinomas showed lost of one *PCPB4* allele. We did not detect normal epithelial cells (alveolar or bronchiolar) with deletion of *PCBP4*, even in proximity to tumor cells.

When we compared the status of *PCBP4* to the presence of αCP-4 in each tumor, a significant correlation (Kendall's τ-b coefficient = 0.612; $P < 0.001$) existed between both parameters, showing a clear association between heterozygosity retention and expression of αCP-4 (Table 2).

We then searched for mutations in the exonic sequence of *PCBP4* (exons 2–13). We analyzed 15 NSCLC (H23, A549, H720, H358, H1264, H460, H157, H226, H2087, H727, H661, Calu-3, H441, HTB-58, and H676) and 9 SCLC (H209, N417, H446, H69, H345, H510, H82, H187, and H774) cell lines and found no mutations.

To evaluate the involvement of other mechanisms in the absence of αCP-4 expression we determined the presence of the αCP-4 mRNA by Northern blot analysis in normal human bronchial epithelial cells and in SCLC and NSCLC cell lines. αCP-4 mRNA was detected in all of them, with some cancer cell lines expressing high message levels. This fact was particularly evident in SCLC cell lines (Fig. 4).

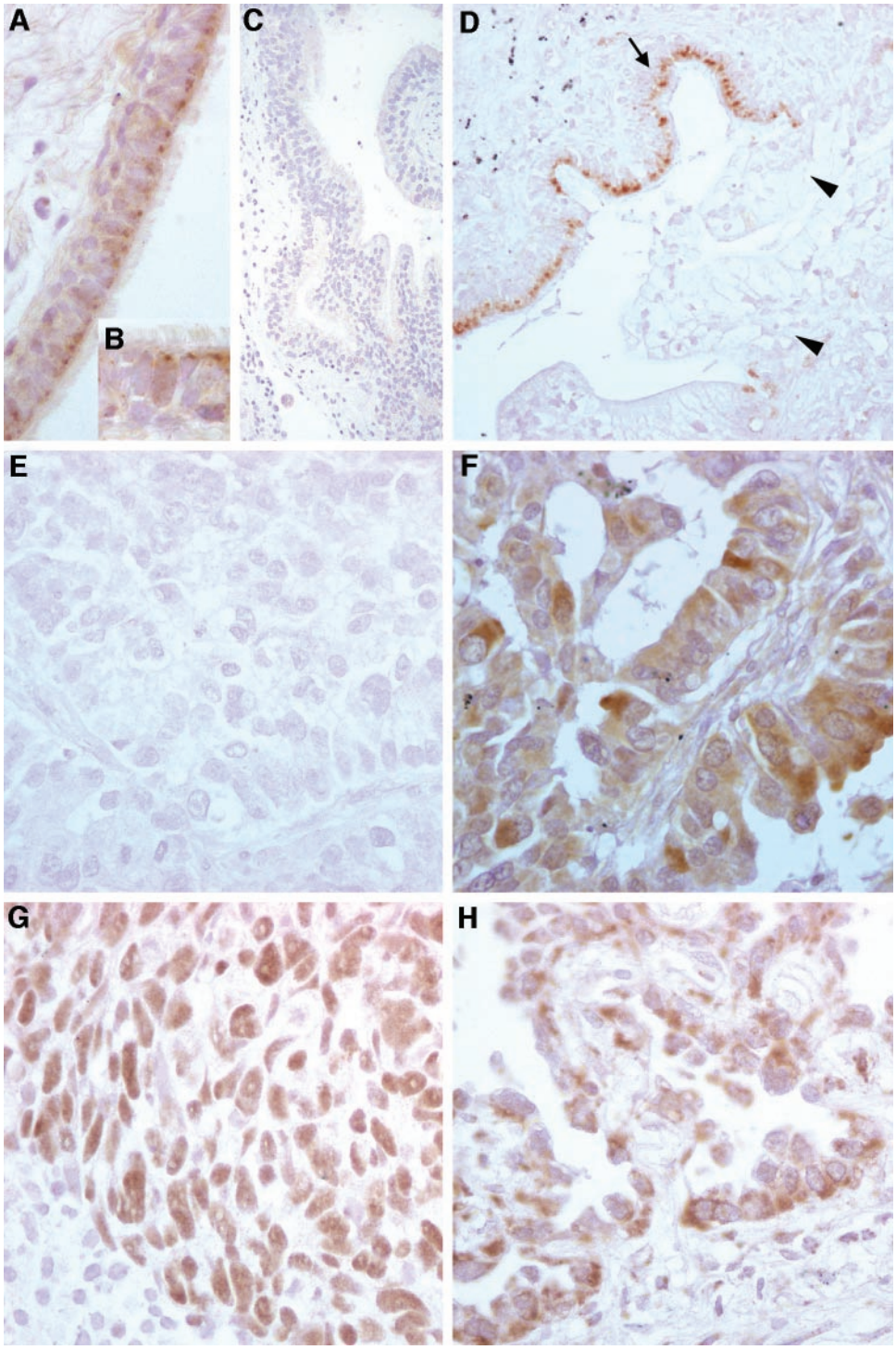

Fig. 2. Immunocytochemical analysis shows that in lung cancer αCP-4 expression is different from αCP-4a expression. *A*, αCP-4 is present in the cytoplasm of bronchiolar epithelium cells. *B*, detail from previous image showing the accumulation of αCP-4 immunoreactivity close to the apical surface of the bronchial cells. *C*, αCP-4 expression is lost in hyperplastic bronchial epithelium. *D*, in the transition from normal bronchiolar epithelium (*arrows*) to tumor (*arrowheads*) a loss of αCP-4 expression can be observed. *E*, an adenocarcinoma with absence of αCP-4 expression. *F*, αCP-4 protein is located in the cytoplasm in a bronchioloalveolar carcinoma. *G*, example of a squamous cell carcinoma with a strong nuclear immunoreactivity for αCP-4a. *H*, expression of αCP-4a in the cytoplasm of cells from a bronchioloalveolar carcinoma. Original magnification of *A*, *E*, *F*, *G*, and *H*: ×500; B: ×1250; *C* and *D*, ×125.

αCP-4a Expression in Lung Cancer. Due to the lack of αCP-4 protein expression in most NSCLC tumors we investigated whether that was also the case for the alternative splice variant αCP-4a. By RT-PCR and using primers flanking the alternatively spliced region at exon 13 (αS-2 and αAS-2; Table 1; Fig. 1), we separately analyzed the expression of the αCP-4 splicing variants, αCP-4 and αCP-4a. Both αCP-4 and αCP-4a mRNA variants were detected in all of the cell lines as 550- and 350-bp bands, respectively (Fig. 5). Their identities were confirmed by cloning and sequencing of the band from H82 cell line. With this technical approach, the expression level of the αCP-4a transcript seemed to be lower than the expression of the αCP-4 transcript. This was confirmed with a semiquantitative real-time RT-PCR analysis carried out in some of the cell lines (Fig. 6). The primer design allowed us to distinguish between the two alternative splice forms (Fig. 1; Table 1). Interestingly, the ratio between both splice forms varied widely between the different cell lines (from 53.6 for H510 to 5.9 for H69 and H1385) suggesting a post-transcriptional regulation. We developed a polyclonal antibody for the specific COOH-terminal sequence of αCP-4a that does not recognize αCP-4. Immunocytochemical analysis in normal lung epithelium demonstrated that αCP-4a expression pattern was similar to what was observed for αCP-4, in which alveoli did not show immunoreactivity,

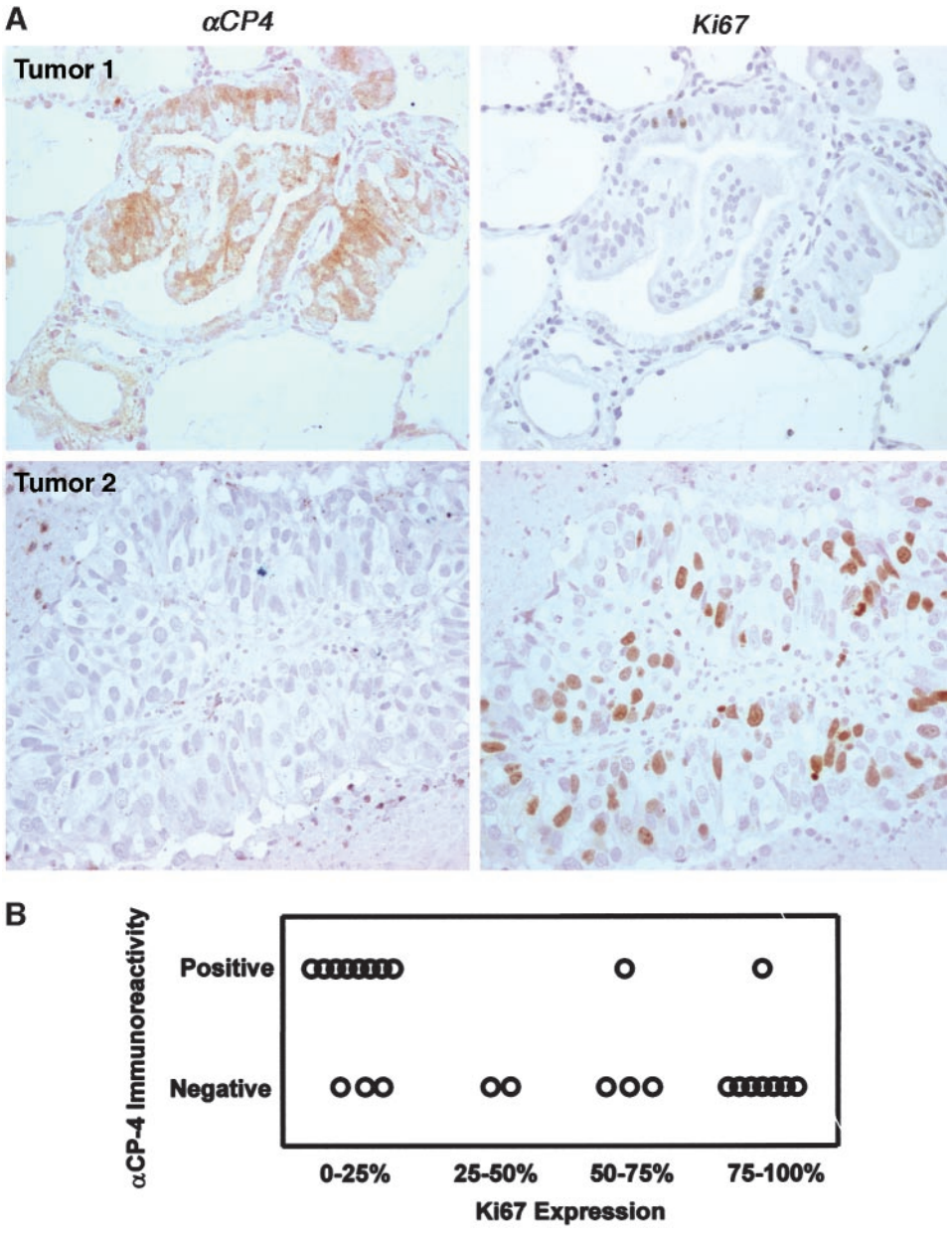

Fig. 3. *A*, immunocytochemical staining for αCP-4 and Ki67 in serial reverse-face sections from two representative non-small cell lung cancers (bronchioloalveolar carcinoma and squamous cell carcinoma) shows an opposite expression of both proteins. Original magnification: ×125. *B*, graph showing the correlation ($n = 25$; Kendall's τ-b coefficient = 0.507; $P = 0.001$) between the expression of αCP-4 and the extension of Ki67 expression in non-small cell lung cancer biopsies.

Table 2 *Contingency table showing αCP-4 immunoreactivity versus PCBP4 deletion*[a]

	PCBP4 LOH[b]		
αCP-4 Immunoreactivity	Normal	Deletion	Total
Positive	9	0	9
Negative	5	7	12
Total	14	7	21

[a] Kendall's τ-b coefficient for correlation was 0.612 ($P < 0.001$).
[b] LOH, loss of heterozygosity.

and bronchioli presented cytoplasmic expression. However, in contrast to what was found for αCP-4 in tumors, αCP-4a was observed in all of the NSCLCs. The localization of the protein widely varied between samples, with tumors showing the protein in the nucleus (Fig. 2*G*), tumors showing cytoplasmic localization (Fig. 2*H*), and tumors expressing the protein in both cell compartments.

Effect of αCP-4 Overexpression on Cell Growth Rate. It has been described previously that MCG10 induces growth suppression in the lung cancer cell line H1299 (11). Although αCP-4 and MCG10 are the same protein, some discrepancies at the NH_2 terminus amino acid sequence has been published (9). Therefore, we wanted to evaluate whether αCP-4 has a similar effect on cell growth regulation. We examined the growth rate of αCP-4- and αCP-4a-inducible transfectants using an 3-(4,5-dimethylthiazol-2-yl)-2,5-diphenyltetrazolium bromide assay. Overexpression of αCP-4 or αCP-4a was induced with

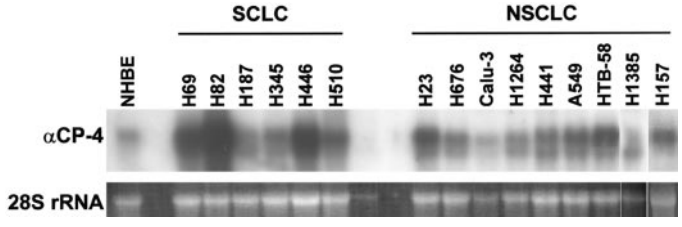

Fig. 4. Northern blot analysis of αCP-4 mRNA expression in normal human bronchial epithelium (*NHBE*) cells, small cell lung cancer (*SCLC*) cell lines and non-small cell lung cancer (*NSCLC*) cell lines. Fifteen μg of total RNA were added per lane, and ethidium bromide staining of 28 S was used to control equal loading and RNA integrity.

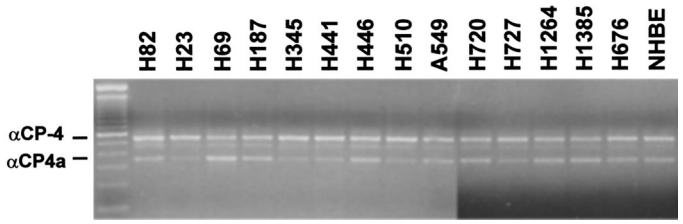

Fig. 5. Reverse transcription-PCR amplification demonstrates the expression of the predicted 550- and 330-pb products corresponding to αCP-4 and αCP-4a, respectively, in normal human bronchial epithelium (*NHBE*) cells, small cell lung cancer cell lines and non-small cell lung cancer cell lines. A subsequence sequencing of both products from H82 mRNA confirmed the identity of the amplified sequences.

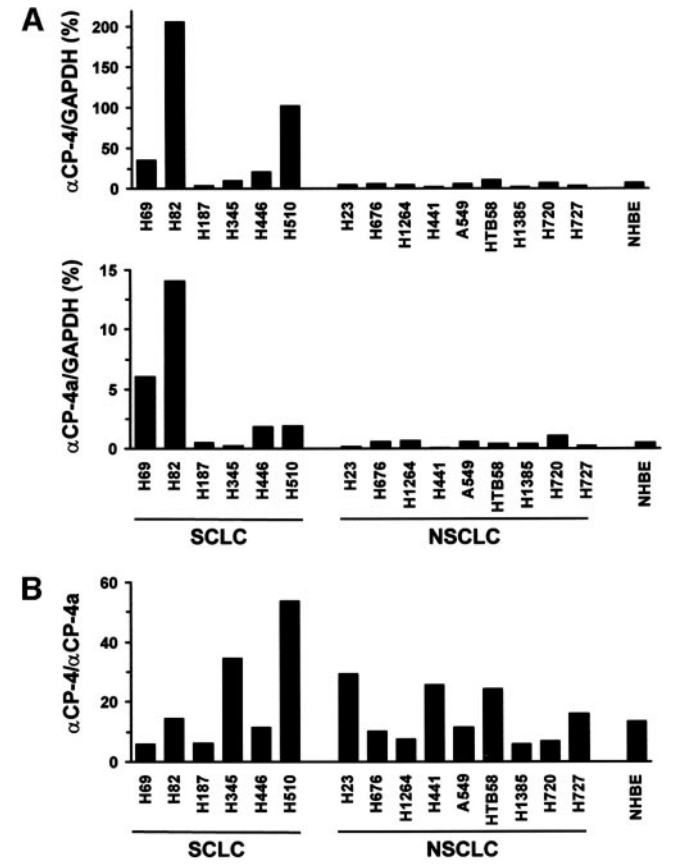

Fig. 6. *A*, real-time PCR for the expression of the alternatively spliced variants αCP-4 and αCP-4a mRNAs in lung cancer cell lines and normal human bronchial epithelium (*NHBE*) cells. The *Y* axis represents the relation between αCP-4 and glyceraldehyde-3-phosphate dehydrogenase (*GAPDH*) mRNA (in percentage). *B*, ratio between the expression of the two alternatively spliced products from the αCP-4 pre-mRNA. *SCLC*, small cell lung cancer; *NSCLC*, non-small cell lung cancer.

1 μg/ml of doxycycline in cells stably transfected with the retroviral vector pLTR containing the complete coding domain sequence for αCP-4 or αCP-4a. The cell rate was measured daily up to 6 days from the beginning of the induction. As observed in Fig. 7*A*, αCP-4 overexpression was capable of reducing cell proliferation after 4 days from induction. This activity was not apparently shared with its alternative splice variant αCP-4a (Fig. 7*B*).

DISCUSSION

Consistent allelic losses at 3p21 strongly support the hypothesis that one or more tumor suppressor genes essential for the development of lung cancer reside within this chromosomal region. Identification of these genes would be crucial to elucidate the molecular mechanisms of lung carcinogenesis. This information will be also useful for the development of molecular-based techniques for early detection of premalignant and malignant cells. Several candidate genes in 3p21 have already been identified as potential tumor suppressors. Most of the research efforts have focused on a 630-kb region defined by homozygous deletion (15–17). In a previous study aimed to identify new potential tumor suppressor genes, 19 genes found in this region and located within a deleted overlap region of 370 kb were tested for mutations and loss of expression in lung cancer (5). Several of them showed reduced or null expression in lung cancer cell lines, although none of them presented a frequent mutation rate. In additional studies, promoter hypermethylation was proven as a common mechanism for the silencing of these genes. Additional functional data have reinforced the role of some of these candidates as tumor suppressor genes (6, 7, 18–22). By using 28 3p markers, Wistuba *et al.* (4) identified other discrete regions of allele loss where other tumor suppressor genes may be located.

In our study we have evaluated the expression of αCP-4, a candidate tumor suppressor gene located at 3p21 and identified recently (10, 11). In accordance with the possible role of αCP-4 as a tumor suppressor for lung tumors, we have detected a frequent lack of αCP-4 expression in NSCLCs, preferentially in squamous cell carcinomas. The loss of αCP-4 expression was associated with poorly differentiated and highly proliferative tumors. Due to the predominant presence of early stage tumors in our series, our data indicate that the alteration

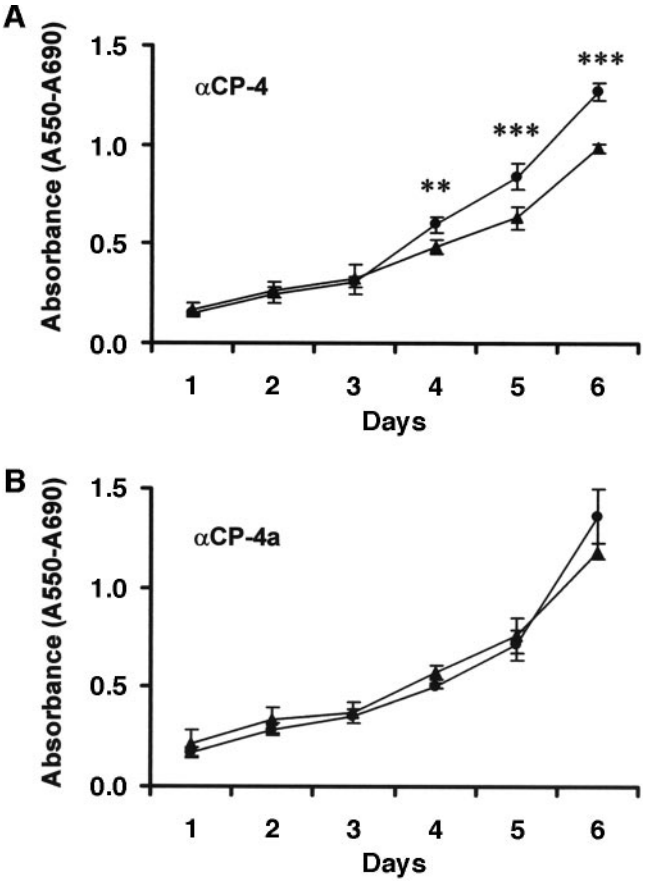

Fig. 7. Effect of αCP-4 and αCP-4a overexpression on H1299 cell growth. Proliferation of αCP-4 (*A*) or αCP4a (*B*) inducible clones was evaluated using an 3-(4,5-dimethylthiazol-2-yl)-2,5-diphenyltetrazolium bromide-based method. Cells were plated (10^3 cells/well) into 96-well plates and cultivated in the presence or absence of doxycycline (1 μg/ml). Data are presented as a function of absorbance (reflecting cell numbers) *versus* time (days after induction). Results are representative of four independent experiments and values are expressed as mean; *bars*, ±SD. **, $P < 0.01$; ***, $P < 0.001$.

in αCP-4 occurs at the earliest clinically detectable phases of lung carcinogenesis. This is supported by the absence of αCP-4 expression in abnormal bronchial lesions such as hyperplasias. As a component of the p53 tumor suppressor pathway it could be argued that the lack of αCP-4 is a consequence of the functional alteration of p53 in the tumor. However, we have not found a correlation between p53 abnormalities (determined as p53 accumulation by immunocytochemistry) and lack of αCP4. Moreover, in some of the studied cases p53 alteration with simultaneous αCP4 expression was found. On the other hand, some tumors with apparently normal p53 (determined by the absence of p53 staining) were negative for αCP4. This indicates that p53 is not a necessary factor for αCP-4 transcription. In addition, the expression of αCP-4a, the alternative splice form, seems to be unaffected by p53 status, as normal bronchial epithelium, premalignant lesions, and tumors showed a strong expression of the protein.

In our study, we have also detected *PCBP4* allele losses in 33% of lung cancer cell lines and primary NSCLCs. Using FISH analysis we compared the number of *PCBP4* signals to the number of chromosome 3 centromeric signals to establish the existence of *PCBP4* deletions. Because no allele-specific typing of the tumors has been performed, the *PCPB4* deletions cannot undoubtedly be associated with LOH. This is particularly true in the case of cell lines showing chromosome 3 polyploidies. However, most primary tumors retain a normal number of chromosome 3 centromeres, indicating that there has not been chromosome 3 duplication (only 1 of 7 specimens with deletion of *PCBP4* had a clear chromosome 3 polysomy). In this case, when we detect the loss of one *PCBP4* signal, LOH is the most likely situation. Therefore, we can conclude that our results demonstrate frequent *PCBP4* deletions most likely associated with LOH at this particular genomic region.

Although 3p allelic losses occur at very early preneoplastic stages of lung cancer, it is accepted that these losses are progressive, and advanced lesions and tumors often have deletions in most of the arm or the entire arm, whereas early lesions have more focal deletions. The NSCLC biopsies studied in our work corresponded preferentially to early stage cases (~90% of the specimens were obtained from patients diagnosed at stages I and II). Therefore, LOH at *PCBP4* seems to be an early change in lung carcinogenesis and not a mere consequence of gross 3p alterations associated with advanced lung cancers. A clear relation between *PCBP4* allele loss and the expression of αCP-4 has been found in the present study where the deletion of *PCBP4* is associated with a loss of αCP-4 expression. In the classical two-hit model for inactivation of a tumor suppressor gene, the loss of one allele is frequently accompanied by an inactivating mutation of the retained allele (23). We have analyzed the presence of mutations in *PCBP4* (exons 2–13) in 24 lung cancer cell lines without detecting any alteration. This is common when searching for a tumor suppressor gene at 3p in lung cancer, where none or very rare mutations have been found in the potential tumor suppressors (5). In fact, there is a general agreement that failing in detecting mutations in a limited number of samples does not necessarily exclude the role of the gene as a tumor suppressor. In sporadic human tumors, events such as transcriptional silencing by promoter hypermethylation or haploinsufficiency are alternative molecular mechanisms for gene inactivation. These processes result in absence or low mRNA levels due to a reduced transcription of the gene. All of the lung cancer cell lines analyzed in our study expressed αCP4 mRNA, even in the absence of one *PCBP4* allele. In fact, in some lung cancer cell lines the mRNA levels were abnormally high when compared with those in primary cultures from normal bronchial cells. Therefore, our data do not suggest a role of promoter hypermethylation or haploinsufficiency in the αCP-4 inactivation. Another mechanism that can affect the expression of a potential tumor suppression gene is the alteration of the RNA processing machinery. Alternative splicing of pre-mRNA is an important regulatory mechanism to control gene expression and to generate proteins with distinct functions. Tumorigenesis and tumor progression have been related to the expression of alternatively spliced mRNAs encoding altered forms of proteins such as cyclin D1, mdm2, Fhit, TSG101, vascular endothelial growth factor, and CD44 (24–29). For that reason, we evaluated the expression of αCP-4a, the other protein derived from *PCBP4* by alternative splicing, in lung cancer. We have been able to demonstrate that αCP-4a mRNA is expressed by lung cancer cell lines and, surprisingly, the protein is present in all lung tumors (although its intracellular location may change from normal to tumors). Considering together both αCP-4 and αCP-4a results, we can speculate that the lack of αCP-4 expression in lung cancer may be due to changes in the processing of the αCP-4 mRNA that lead to a predominant expression of αCP-4a.

Only speculation can be made about the mechanisms responsible for the altered processing of the αCP-4 mRNA. Many intracellular proteins are involved in the processing of the mRNA, and any alteration in their expression or function in cancer may change the processing of mRNAs such as that for αCP-4. Heterogeneous nuclear ribonucleoproteins are RNA binding proteins involved in mRNA splicing, localization, stabilization, nuclear-cytoplasm transport, and translation. In NSCLCs we have found a progressive increase in heterogeneous nuclear ribonucleoproteins A1, A2/B1, C1/C2, and K expression from normal lung epithelium to hyperplastic lesions and tumors (30). Other heterogeneous nuclear ribonucleoproteins proteins and RNA binding proteins have been related to tumors (29, 31–35). Altered expression of alternative splicing regulatory factors has also been reported in *in vitro* models of cellular transformation (36). The modifications in the expression of these RNA processing proteins in lung cancer may alter the fate of some mRNAs important for normal cell physiology giving rise to proteins associated with tumor formation and/or maintenance. For example, Bcl-xL and Bcl-xS are splice variants produced by alternative splicing of Bcl-x pre-mRNA. Whereas Bcl-xL is antiapoptotic, Bcl-xS has been shown to produce cell death (37). In many malignancies, Bcl-xL is the predominant form, with low or undetectable levels of Bcl-xS (38–41).

Our knowledge on the cellular activity of αCP-4 is limited. In the search for novel cellular p53 target genes, *MCG10* was identified as a gene specifically induced by wild-type p53 and DNA damage. In a lung cancer cell line (H1299) that inducibly overexpressed MCG10 it was found that this protein was able to increase apoptosis and cell cycle arrest in G_2-M (11). All of these data suggested that MCG10 may be a potential mediator of p53 tumor suppression. MCG10 and αCP-4 are the same protein, although MCG10 is truncated at the NH_2 terminus. We have now confirmed the growth inhibition effect mediated by αCP4 overexpression. It can be suggested that the loss of αCP-4 expression found in the NSCLC biopsies would result in stimulation of cell proliferation with diminution of apoptosis. This would participate in the development of the malignant phenotype. This is in agreement with the correlation that exists between the lack of αCP-4 expression and the proliferative status of the tumor. The relevance of the loss of this protein in the prognosis of lung cancer merits examination.

Although nothing is known about the molecular mechanisms that mediate αCP-4 activity, it is known that disruption of the polycytidylic acid binding domains is necessary for inducing apoptosis and cell cycle arrest (11). The best-known members of the αCP family are αCP-1 and αCP-2, also known as heterogeneous nuclear ribonucleoproteins E1/E2 or PCBP1/2. These proteins are involved

in several biological processes mediated by their binding to C-rich single-strand motif in the RNA (9). These proteins are linked to mRNA stabilization, translational activation, and translational silencing. Through the binding to specific mRNAs, αCP-4 may control the fate of specific mRNAs, regulating the cellular processes in which their proteins are involved (i.e. apoptosis and cell cycle arrest). αCP-4a, the alternatively spliced variant of αCP-4, differs in the primary COOH-terminal sequence from αCP-4. αCP-4a is shorter and does not contain potentially important αCP-4 motifs such as proline-rich domains, a nuclear export signal and a nuclear localization signal (11). Interestingly, our data suggest a distinct effect of αCP-4 and αCP-4a on cell growth. Whereas αCP-4 expression is associated with reduced cell proliferation, in our study, αCP-4a overexpression did not apparently affect growth rate. Considering also its expression and location in lung tumors, this result strongly suggests that *in vivo* αCP-4a activity is different from that of αCP-4.

Although our data support that αCP-4 acts as a tumor suppressor protein, more detailed functional analyses such as gene transfer and gene disruption should be performed to clarify the role of αCP-4 in carcinogenesis. Additional studies must also be conducted to demonstrate that the replacement of its expression suppresses tumorigenicity *in vivo*. These functional evidences are required for the establishment of αCP-4 as a tumor suppressor gene of which the inhibition is important for malignant transformation. It should also be interesting to determine the involvement of the splice variant αCP-4a in lung carcinogenesis. Besides, an understanding of the regulatory mechanisms of alternative splicing occurring along with neoplastic transformation may help to elucidate some of the causes of this and other abnormal gene expressions in lung cancer. Understanding these mechanisms might also pave the way to restoring the function of tumor suppressor genes affected by splicing alterations.

In conclusion, our results, together with previous data implicating MCG10 in apoptosis and cell cycle arrest (11), suggest a role of αCP-4 as a new tumor suppressor associated with lung carcinogenesis. Among the abnormalities described in our work, we have found frequent *PCBP4* deletions in lung cancer. In the case of a NSCLC series, these deletions were associated with lack of αCP-4 expression, whereas αCP-4a was expressed in all of the tumors. Our data suggest that dysregulation of αCP4 mRNA metabolism may account for this modification, creating an abnormal expression pattern, which helps cancer growth. Additional studies on the αCP-4 functions and gene alterations would contribute to the elucidation of the molecular mechanisms involved in lung malignant transformation and would help in the improvement of prevention, detection, and treatment strategies for lung cancer.

ACKNOWLEDGMENTS

We thank Amaya Lavin for technical assistance and Dr. Iñaki Martin-Subero for helping us with the FISH technique. We also thank Dr. Wenceslao Torre, Dr. Javier Zulueta, Dr. Maria Jose Pajares, Natalia Rey, and Usua Montes for their work in the collection of the NSCLC biopsies.

REFERENCES

1. Sundaresan V, Ganly P, Hasleton P, et al. p53 and chromosome 3 abnormalities, characteristic of malignant lung tumours, are detectable in preinvasive lesions of the bronchus. Oncogene 1992;7:1989–97.
2. Hung J, Kishimoto Y, Sugio K, et al. Allele-specific chromosome 3p deletions occur at an early stage in the pathogenesis of lung carcinoma. J Am Med Assoc 1995;273:558–63.
3. Wistuba II, Lam S, Behrens C, et al. Molecular damage in the bronchial epithelium of current and former smokers. J Natl Cancer Inst 1997;89:1366–73.
4. Wistuba II, Behrens C, Virmani AK, et al. High resolution chromosome 3p allelotyping of human lung cancer and preneoplastic/preinvasive bronchial epithelium reveals multiple, discontinuous sites of 3p allele loss and three regions of frequent breakpoints. Cancer Res 2000;60:1949–60.
5. Lerman MI, Minna JD. The 630-kb lung cancer homozygous deletion region on human chromosome 3p21.3: identification and evaluation of the resident candidate tumor suppressor genes. The International Lung Cancer Chromosome 3p21.3 Tumor Suppressor Gene Consortium. Cancer Res 2000;60:6116–33.
6. Dammann R, Li C, Yoon JH, Chin PL, Bates S, Pfeifer GP. Epigenetic inactivation of a RAS association domain family protein from the lung tumour suppressor locus 3p21.3. Nat Genet 2000;25:315–9.
7. Tomizawa Y, Sekido Y, Kondo M, et al. Inhibition of lung cancer cell growth and induction of apoptosis after reexpression of 3p21.3 candidate tumor suppressor gene SEMA3B. Proc Natl Acad Sci USA 2001;98:13954–9.
8. Sutherland LC, Lerman M, Williams GT, Miller BA. LUCA-15 suppresses CD95-mediated apoptosis in Jurkat T cells. Oncogene 2001;20:2713–9.
9. Makeyev AV, Liebhaber SA. The poly(C)-binding proteins: a multiplicity of functions and a search for mechanisms. RNA 2002;8:265–78.
10. Makeyev AV, Liebhaber SA. Identification of two novel mammalian genes establishes a subfamily of KH-domain RNA-binding proteins. Genomics 2000;67:301–16.
11. Zhu J, Chen X. MCG10, a novel p53 target gene that encodes a KH domain RNA-binding protein, is capable of inducing apoptosis and cell cycle arrest in G(2)-M. Mol Cell Biol 2000;20:5602–18.
12. Chkheidze AN, Liebhaber SA. A novel set of nuclear localization signals determine distributions of the alphaCP RNA-binding proteins. Mol Cell Biol 2003;23:8405–15.
13. Davis LG, Kuehl WM, Battey JM. Basic methods in Molecular Biology, 2 edition. Norwalk, CT: Appleton & Lange, 1994:322–28.
14. Watsuji T, Okamoto Y, Emi N, Katsuoka Y, Hagiwara M. Controlled gene expression with a reverse tetracycline-regulated retroviral vector (RTRV) system. Biochem Biophys Res Commun 1997;234:769–73.
15. Daly MC, Xiang RH, Buchhagen D, et al. A homozygous deletion on chromosome 3 in a small cell lung cancer cell line correlates with a region of tumor suppressor activity. Oncogene 1993;8:1721–9.
16. Kok K, van den Berg A, Veldhuis PM, van der Veen AY, et al. A homozygous deletion in a small cell lung cancer cell line involving a 3p21 region with a marked instability in yeast artificial chromosomes. Cancer Res 1994;54:4183–7.
17. Wei MH, Latif F, Bader S, et al. Construction of a 600-kilobase cosmid clone contig and generation of a transcriptional map surrounding the lung cancer tumor suppressor gene (TSG) locus on human chromosome 3p21.3: progress toward the isolation of a lung cancer TSG. Cancer Res 1996;56:1487–92.
18. Burbee DG, Forgacs E, Zochbauer-Muller S, et al. Epigenetic inactivation of RASSF1A in lung and breast cancers and malignant phenotype suppression. J Natl Cancer Inst 2001;93:691–9.
19. Brambilla E, Constantin B, Drabkin H, Roche J. Semaphorin SEMA3F localization in malignant human lung and cell lines: A suggested role in cell adhesion and cell migration. Am J Pathol 2000;156:939–50.
20. Ji L, Nishizaki M, Gao B, et al. Expression of several genes in the human chromosome 3p21.3 homozygous deletion region by an adenovirus vector results in tumor suppressor activities in vitro and in vivo. Cancer Res 2002;62:2715–20.
21. Kondo M, Ji L, Kamibayashi C, et al. Overexpression of candidate tumor suppressor gene FUS1 isolated from the 3p21.3 homozygous deletion region leads to G1 arrest and growth inhibition of lung cancer cells. Oncogene 2001;20:6258–62.
22. Timmer T, Terpstra P, van den Berg A, et al. A comparison of genomic structures and expression patterns of two closely related flanking genes in a critical lung cancer region at 3p21.3. Eur J Hum Genet 1999;7:478–86.
23. Knudson AG Jr, Hethcote HW, Brown BW. Mutation and childhood cancer: a probabilistic model for the incidence of retinoblastoma. Proc Natl Acad Sci USA 1975;72:5116–20.
24. Hosokawa Y, Gadd M, Smith AP, Koerner FC, Schmidt EV, Arnold A. Cyclin D1 (PRAD1) alternative transcript b: full-length cDNA cloning and expression in breast cancers. Cancer Lett 1997;113:123–30.
25. Sigalas I, Calvert AH, Anderson JJ, Neal DE, Lunec J. Alternatively spliced mdm2 transcripts with loss of p53 binding domain sequences: transforming ability and frequent detection in human cancer. Nat Med 1996;2:912–7.
26. Sozzi G, Veronese ML, Negrini M, et al. The FHIT gene 3p14.2 is abnormal in lung cancer. Cell 1996;85:17–26.
27. Oh Y, Proctor ML, Fan YH, et al. TSG101 is not mutated in lung cancer but a shortened transcript is frequently expressed in small cell lung cancer. Oncogene 1998;17:1141–8.
28. Cheung N, Wong MP, Yuen ST, Leung SY, Chung LP. Tissue- specific expression pattern of vascular endothelial growth factor isoforms in the malignant transformation of lung and colon. Hum Pathol 1998;29:910–4.
29. Stickeler E, Kittrell F, Medina D, Berget SM. Stage-specific changes in SR splicing factors and alternative splicing in mammary tumorigenesis. Oncogene 1999;18:3574–82.
30. Pino I, Pio R, Toledo G, et al. Altered patterns of expression of members of the heterogeneous nuclear ribonucleoprotein (hnRNP) family in lung cancer. Lung Cancer 2003;41:131–43.

31. Perrotti D, Bonatti S, Trotta R, et al. TLS/FUS, a pro-oncogene involved in multiple chromosomal translocations, is a novel regulator of BCR/ABL-mediated leukemogenesis. EMBO J 1998;17:4442–55.
32. Yang L, Embree LJ, Hickstein DD. TLS-ERG leukemia fusion protein inhibits RNA splicing mediated by serine-arginine proteins. Mol Cell Biol 2000;20: 3345–54.
33. Kovar H, Jug G, Hattinger C, et al. The EWS protein is dispensable for Ewing tumor growth. Cancer Res 2001;61:5992–7.
34. Iervolino A, Santilli G, Trotta R, et al. hnRNP A1 nucleocytoplasmic shuttling activity is required for normal myelopoiesis and Bcr/Abl leukemogenesis. Mol Cell Biol 2002;22:2255–66.
35. Gouble A, Grazide S, Meggetto F, Mercier P, Delsol G, Morello D. A new player in oncogenesis: AUF1/hnRNP D overexpression leads to tumorigenesis in transgenic mice. Cancer Res 2002;62:1489–95.
36. Maeda T, Hiranuma H, Jikko A. Differential expression of the splicing regulatory factor genes during two-step chemical transformation in a BALB/3T3-derived cell line, MT-5. Carcinogenesis 1999;20:2341–4.
37. Boise LH, Gonzalez-Garcia M, Postema CE, et al. Bcl-x, a bcl-2-related gene that functions as a dominant regulator of apoptotic cell death. Cell 1993;74:597–608.
38. Dole MG, Jasty R, Cooper MJ, Thompson CB, Nunez G, Castle VP. Bcl-xL is expressed in neuroblastoma cells and modulates chemotherapy-induced apoptosis. Cancer Res 1995;55:2576–82.
39. Xerri L, Parc P, Brousset P, et al. Predominant expression of the long isoform of Bcl-x (Bcl-xL) in human lymphomas. Br J Haematol 1996;92:900–6.
40. Gazzaniga P, Gradilone A, Silvestri I, et al. Variable levels of bcl-2, bcl-x and bax mRNA in bladder cancer progression. Oncol Rep 1998;5:901–4.
41. Miyamoto Y, Hosotani R, Wada M, et al. Immunohistochemical analysis of Bcl-2, Bax, Bcl-X, and Mcl-1 expression in pancreatic cancers. Oncology 1999;56:73–82.